COMMUNICATION

Supplementary information

Operando Structure Degradation Study of PbS Quantum Dot Solar Cells

Wei Chen†,[a,b] Renjun Guo†,[a] Haodong Tang,†,[b] Kerstin S. Wienhold,[a] Nian Li,[a] Zhengyan Jiang,[c] Jun Tang,[c] Xinyu Jiang,[a] Lucas P. Kreuzer,[a] Haochen Liu,[b] Matthias Schwartzkopf,[d] Xiao Wei Sun,[b,e] Stephan V. Roth,[d,f] Kai Wang*,[b,e] Baomin Xu,*[c,e] Peter Müller-Buschbaum*[a,g]

a. Physik Department, Lehrstuhl für Funktionelle Materialien, Technische Universität München, James-Franck-Straße 1, 85748 Garching, Germany. E-mail: muellerb@ph.tum.de

b. Guangdong-Hong Kong-Macao Joint Laboratory for Photonic-Thermal-Electrical Energy Materials and Devices, and Department of Electrical and Electronic Engineering, Southern University of Science and Technology, Shenzhen 518055, China. E-mail: wangk@sustech.edu.cn

c. Department of Materials Science and Engineering, Southern University of Science and Technology (SUSTech), Xueyuan Blvd. 1088, 518055 Shenzhen, China. E-mail: xubm@sustech.edu.cn

d. Deutsches Elektronen-Synchrotron DESY, Notkestraße 85, 22607 Hamburg, Germany

e. Key Laboratory of Energy Conversion and Storage Technologies (Southern University of Science and Technology), Ministry of Education, Shenzhen 518055, China

f. KTH Royal Institute of Technology, Department of Fibre and Polymer Technology, Teknikringen 56-58, SE-100 44 Stockholm, Sweden

g. Heinz Maier-Leibnitz Zentrum (MLZ), Technische Universität München, Lichtenbergstraße. 1, 85748 Garching, Germany

Experimental details.

Materials synthesis: The synthesis method was following previous literature [S1] with slight modifications, briefly described as follows: Lead oxide (PbO, 1.1 g) was dissolved into the mixed solvent of oleic acid (OA, $C_{18}H_{34}O_2$, 7 mL) and octadecene (ODE, C18H36, 20 mL). After purification by degassing and injecting inert gas (Ar), the mixture was heated up to 150 °C to obtain the lead precursor solvent ($Pb(OA)_2$). Then the temperature was set to 100 °C and a 6 hours evacuation was applied to further purify the reaction solvent. After evacuation for 6 hours, the flask was refilled with Ar. The temperature was maintained at 80 °C. Bis(trimethylsilyl)sulfide [$(TMS)_2S$, 530 µL] was used as S precursor and rapidly injected into the lead precursor to trigger the nucleation and growth of the PbS nanocrystals. The reaction lasted for 90 s and then was terminated by ice-bath and simultaneous injection 10 mL

cool octane. After the purification process, induced by adding with acetone and high-speed centrifugation, the QDs were dispersed in octane with the desired concentration of 50 mg/mL for the deposition and the ink fabrication.

QD-ink fabrication: QD-ink fabrication was mainly following previous work by Liu *et al*.[S2] Lead iodide (PbI_2, Sigma (211168), 461 mg), lead bromide ($PbBr_2$, Alfa Aesar (35703.03), 75 mg) and ammonium acetate (AA, 35 mg) were dissolved into 20 mL *N,N*-dimethylformamide (DMF) as the ink precursor. 20 mL PbS QDs (10 mg/mL) was added into the ink precursor and then a phase separation was seen after shaking the mixture for 1 min. Thereby, QDs were transferred from the octane phase to the DMF phase. QDs in the DMF were washed 3 times by octane to completely remove the oleic acid and then precipitated by mixing with the same volume of toluene and centrifugation. After vacuum-drying treatment, the QD-ink became pellets and was re-dissolved in *n*-butylamine (BTA) with a concentration of 200 mg/mL.

Device fabrication: The device fabrication was mainly following previous work with modifications.[S2] The clean laser-patterned ITO (Lumtec, LT-G001PT) substrates were treated for 10 min with O_2 plasma to improve the wettability of the diluted SnO_2 nanoparticles solution. The SnO_2 nanoparticle, 15% in H_2O colloidal dispersion (Alfa Aesar, 44592.36), was diluted into deionized water with the ratio of 1: 3 ratio and the obtained solution was shaken for over 3 hours. The solvent was deposited on the substrates by spin-coating (3000 rpm for 30 s) and then the layer was annealed at 150 °C for 30 min to form the electron transport layer (ETL). 120 µL QD ink (200 mg/mL) was deposited on the SnO_2 layer to obtain the active layer by spin-coating (2600 rpm for 30 s). 150 µL 50 mg/mL oleic acid capped PbS QDs were spin-coated (3000 rpm for 10 s) on the QD-ink layer. 1,2-Ethanedithiol (EDT) in acetonitrile (0.02 % v:v) was applied afterward to performed the ligand exchange treatment. Then pure acetonitrile was used for rinsing the solid twice and removing the residuals. The deposition of OA capped QDs and the solid-state ligand exchange processes were repeated once to form the final hole transport layer. 80 nm gold layer was deposited via thermal evaporation on the EDT-QD layer to finish the cell fabrication. ZnO ETL based solar cells are fabricated following a similar protocol but using the ZnO ink instead of the SnO_2 ink. ZnO ink was purchased from Sigma-Aldrich, and it was used straight forward as received with the same spin-coating parameters with SnO_2 layer.

***Operando* experiment in synchrotron:** The *operando* experiment was carried out at the MiNaXS beamline P03 of the PETRA III synchrotron (DESY, Hamburg).[S3] The X-ray photon energy was set to 11.65 keV, which corresponded to a wavelength of 1.06 Å. The GISAXS detector was a Pilatus 1M (Dectris Inc.) with a pixel size of 172 µm and a frame rate of 10 Hz. The sample-detector distance was 2324 mm. The Pilatus 300K was used as the GIWAXS detector with a sample-detector distance of 168 mm. The micro-focused beam size was about 30 µm × 20 µm. The solar cell was installed into an evacuated chamber with a pressure of 10^{-2} mbar. The inner temperature was stabilized at 15 °C by a water-cooling system to prevent a potential structure change provoked by temperature. The solar simulator was used to provide the illumination (100 mW/cm^2). The current-voltage (IV) curves as a function of time were recorded by source meter Keithley (2400) with an acquisition frequency of one scanning per 120 s. The whole measurement was performed for 90 min.

In-house GISAXS/GIWAXS measurements: The static GISAXS/GIWAXS measurements were carried out at the Ganesha 300XL SAXS instrument with an 8 keV Cu-K_α X-ray source and beam size of 100 µm × 100 µm. The samples were installed in an evacuated chamber (1.2×10^{-3} Pa), and the detector was Pilatus 300 K (Dectris Inc.). The sample-detector distances were 1045 mm for GISAXS and 95.7 mm for GIWAXS measurements, respectively. The degradation conditions for static QD solid samples were the same as in the *operando* experiment.

Details for SCAPS Simulation:[S4,S5] Detailed parameters for establishing the simulation are given in Table S1. We applied energy disorders to determine their corresponding N_t. For the simulation of a fresh sample, we did not apply N_t. For the device sample after the burn-in test, we introduced a new defect level with Gaussian distribution, where N_t total (1/cm) was set to 1.6×10^{15}, and the relative N_t peak was 8.8×10^{15} for simulating the disordered energy distribution. However, different levels of energy disorder active layer will affect the carrier mobility, recombination rate, and ultimately bring different defect density (N_t). Hence, for the modified situation, both hole/electron mobilities were increased to 6×10^{-2} $cm^2/V\cdot s$. Correlated interface parameters can be found in Table S2. The device architecture sketch and the simulated JV curves are presented in Fig. S17.

REFERENCES:

[S1] J. Zhang, R. W. Crisp, J. Gao, D. M. Kroupa, M. C. Beard and J. M. Luther, *J. Phys. Chem. Lett.*, **2015**, 6, 1830-1833.

[S2] M. Liu, O. Voznyy, R. Sabatini, F. P. Garcia de Arquer, R. Munir, A. H. Balawi, X. Lan, F. Fan, G. Walters, A. R. Kirmani, S. Hoogland, F. Laquai, A. Amassian and E. H. Sargent, *Nat. Mater.*, **2017**, 16, 258-263.

[S3] A. Buffet, A. Rothkirch, R. Dohrmann, V. Körstgens, M. M. Abul Kashem, J. Perlich, G. Herzog, M. Schwartzkopf, R. Gehrke, P. Müller-Buschbaum, S. V. Roth, *J. Synchrotron Radiat.,* **2012**, 19, 647.

[S4] M. Burgelman, P. Nollet and S. Degrave, *Thin Solid Films*, 2000, 361-362, 527-532.

[S5] X. Yang, J. Yang, J. Khan, H. Deng, S. Yuan, J. Zhang, Y. Xia, F. Deng, X. Zhou, F. Umar, Z. Jin, H. Song, Chun Cheng, M. Sabry, J. Tang, *Nano-Micro Lett*., **2020**, 12, 37.

Other useful figures:

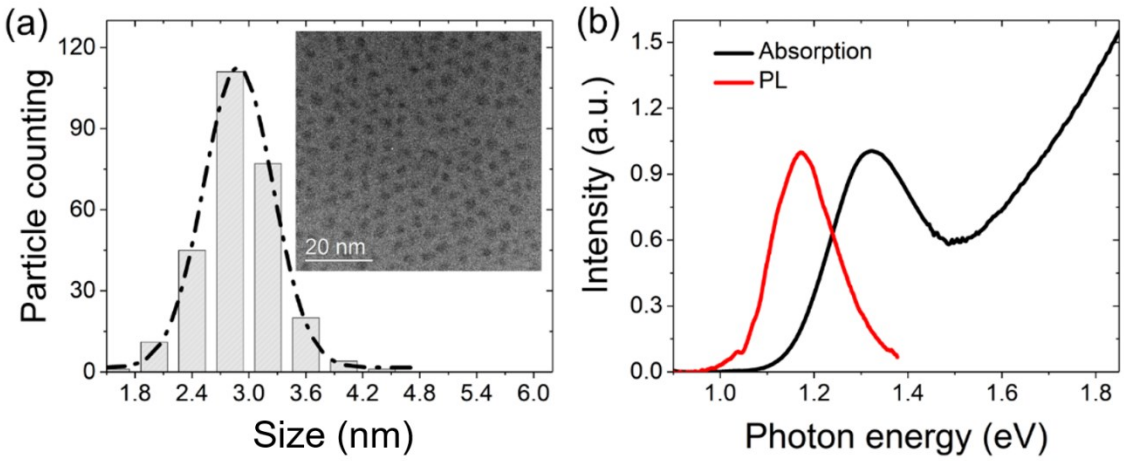

Fig. S1 (a) Particle size analysis and inset TEM image suggest the average diameter of the QDs is 2.88 ± 0.36 nm. (b) Absorption (black) and emission spectra (red) of the QDs in octane.

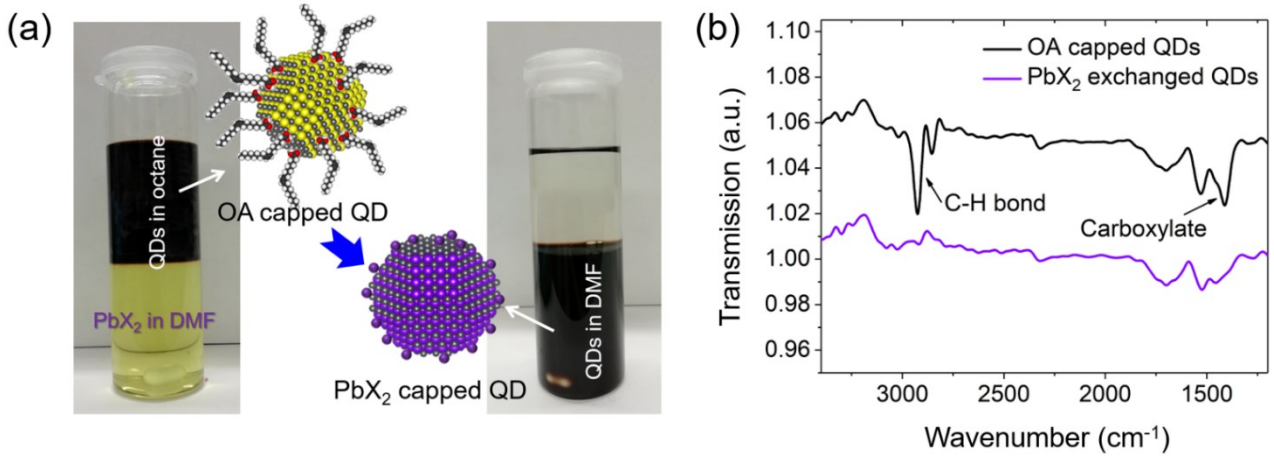

Fig. S2 (a) Photographs describe the phase transfer of QDs from the octane phase to the DMF phase. (b) FTIR spectra indicate the complete removal of oleic acid ligand on the QDs in the ink phase. The spectra are shifted for clarity.

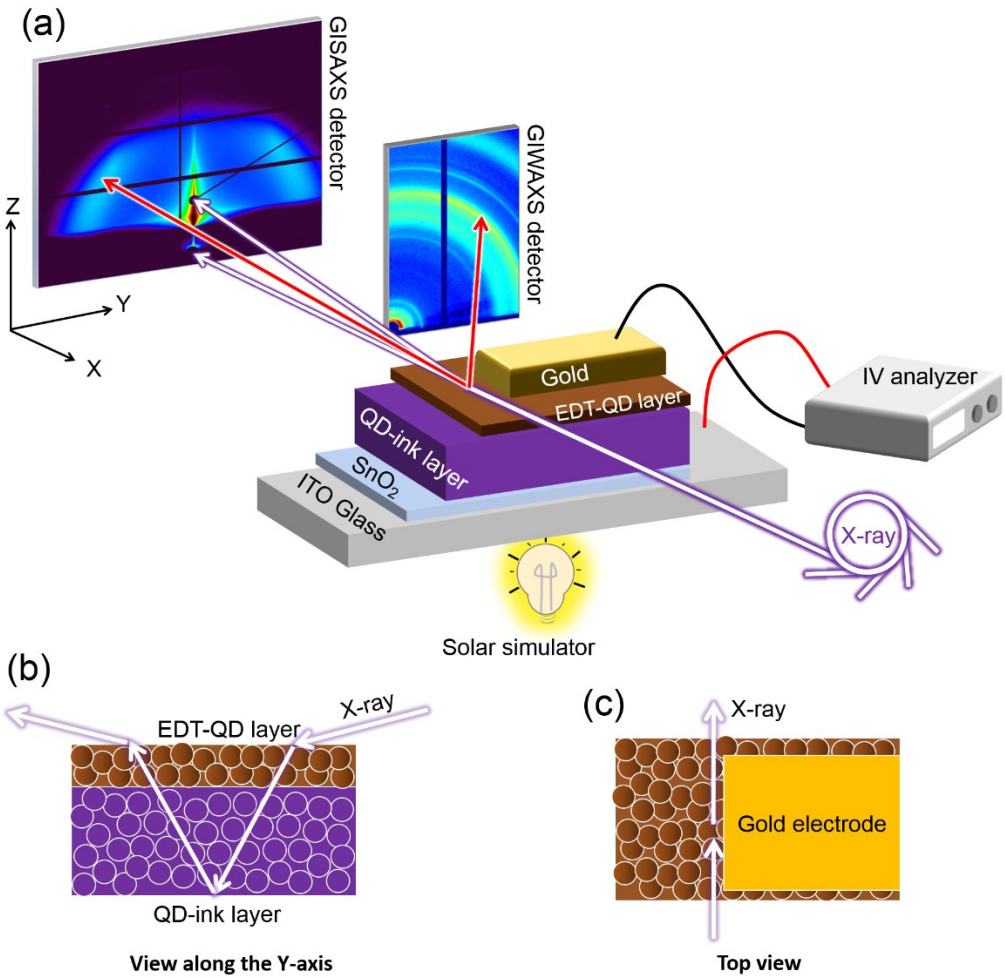

Fig. S3 (a) Schematic of the *operando* structure degradation study of QD based solar cells using synchrotron based GISAXS/GIWAXS. The device diagram of QD solar cells and the schematic for X-ray penetration of the QDs are provided as (b) the view from the Y-axis and (c) the top view.

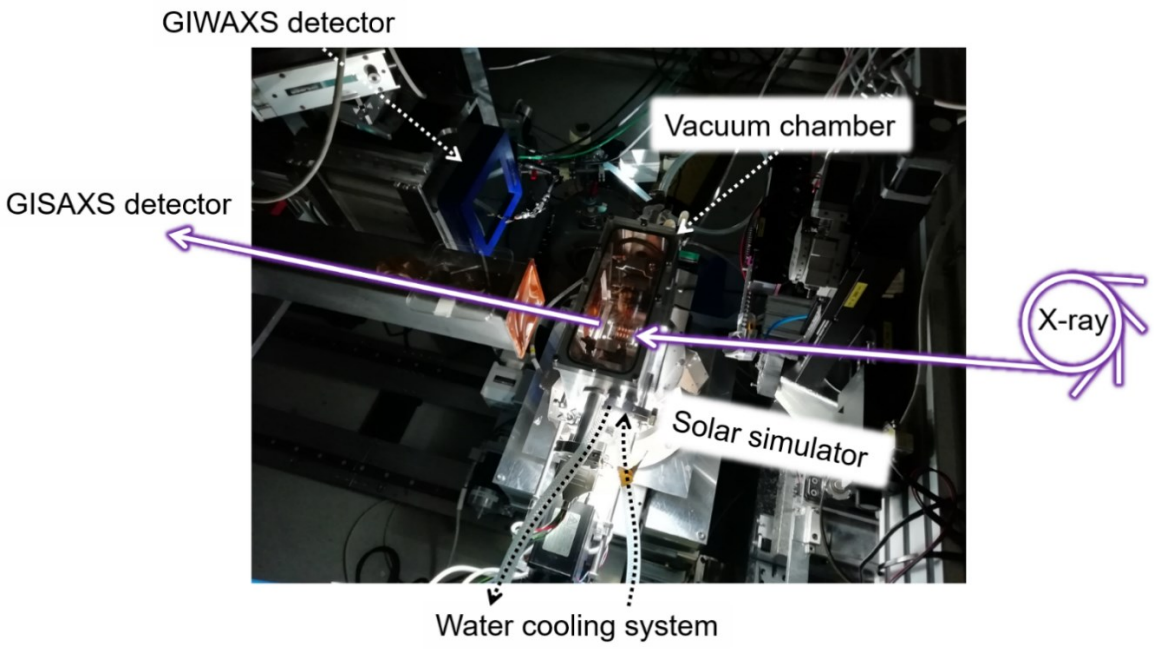

Fig. S4 Photograph of the *operando* setup installed at the synchrotron beamline with both GISAXS and GIWAXS detector, a pocket solar simulator, a water-cooling system, a vacuum chamber, an IV analyzer (source meter Keithley).

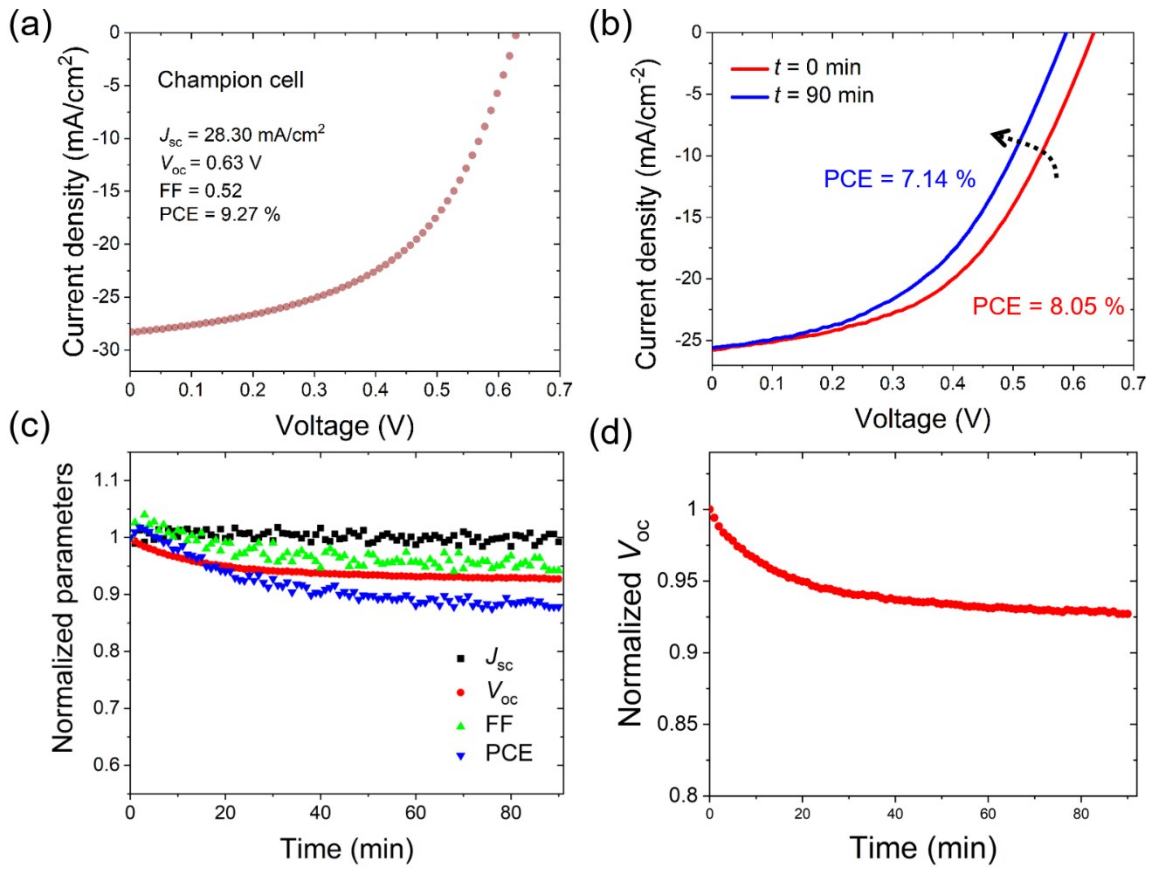

Fig. S5 (a) JV curve of SnO_2 based QD solar cell with a champion PCE of 9.27 %. (b) Additional JV curves of a new batch of device before and after the burn-in test. (c) Normalized parameters of the device performance under the burn-in test. (d)Normalized V_{oc} evolution during the burn-in test.

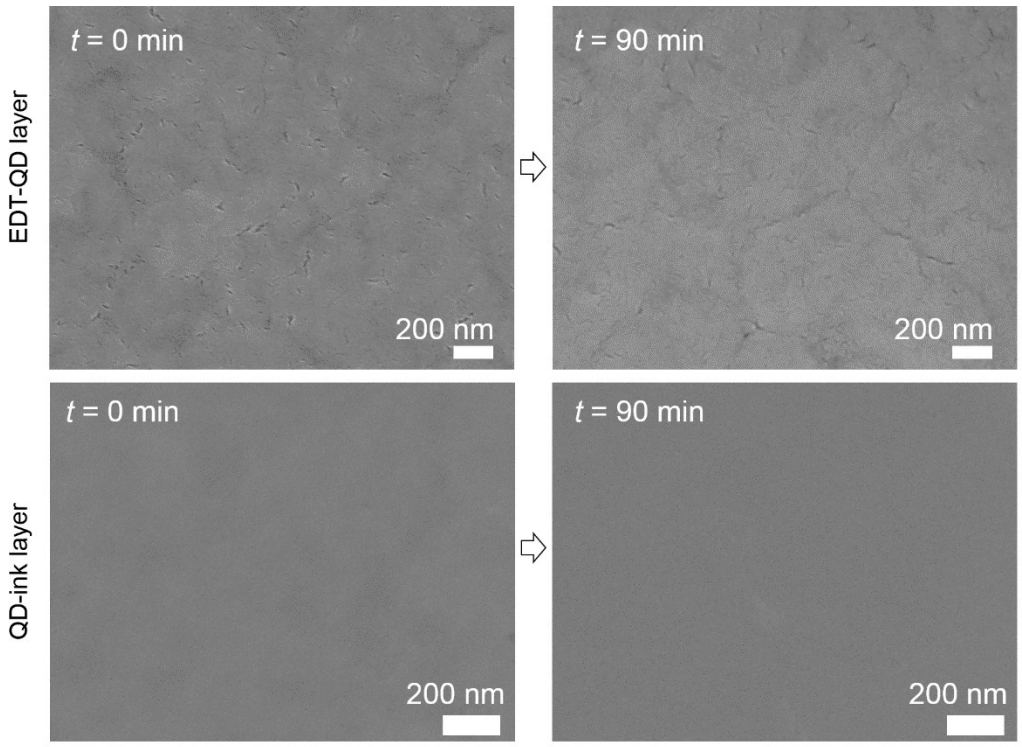

Fig. S6 Surface morphologies of the (top) QD-ink layer and (bottom) EDT-QD layer on glass substrate (left) before and (right) after degradation (under the same illumination degradation conditions as the *operando* experiment).

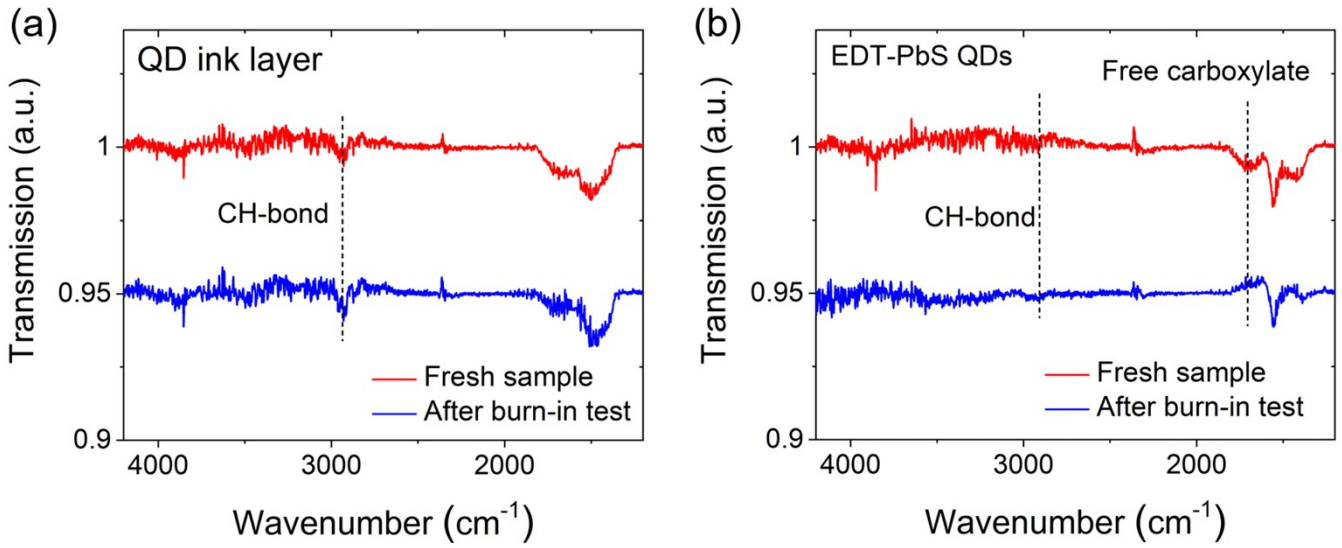

Fig. S7 FTIR spectra of the QD solids before and after the burn-in test aging. (a) QD-ink layer, (b) EDT-PbS layer, in which the "free carboxylate group" peak appears at ~1700 cm-1 getting vanished after burn-in test attributing to the re-bonding of carboxylate group on the surface of PbS QDs in the EDT-PbS layer.

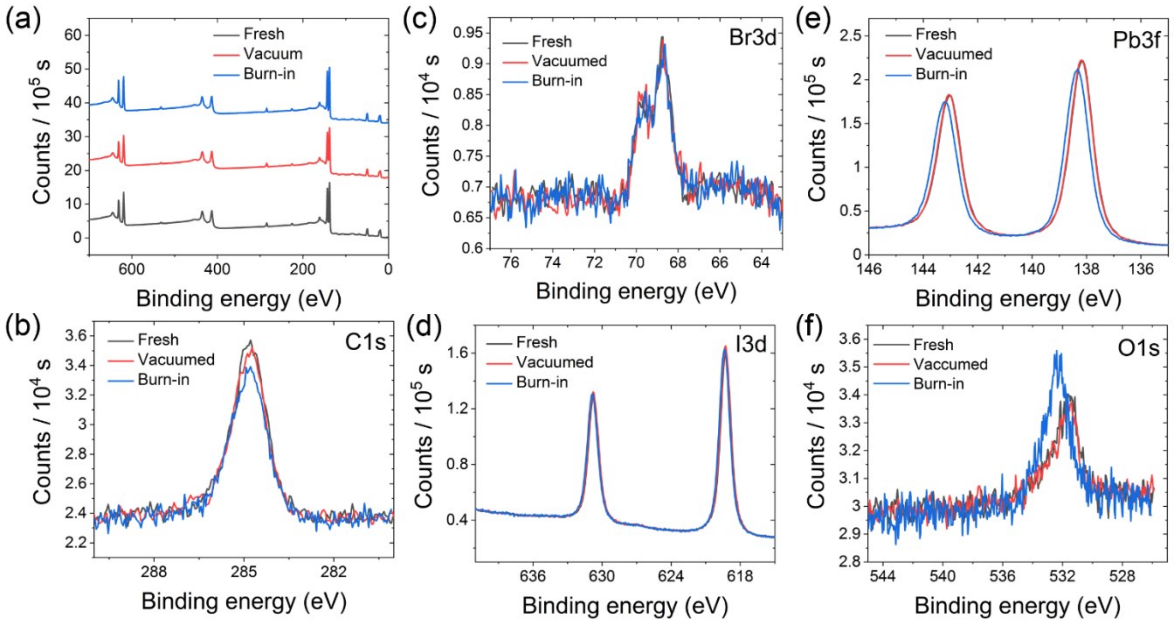

Fig. S8 (a) Survey scan XPS spectra of the QD solids and specific scans for (b) C 1s, (c) Br 3d, (d) I 3d, (e) Pb 4f and (f) O 1s peaks. The peak shifts of Pb 3f and O 1s towards higher binding energies indicate a slight surface oxidation ($PbSO_3$ transforms into $PbSO_4$) under light illumination in the burn-in test.

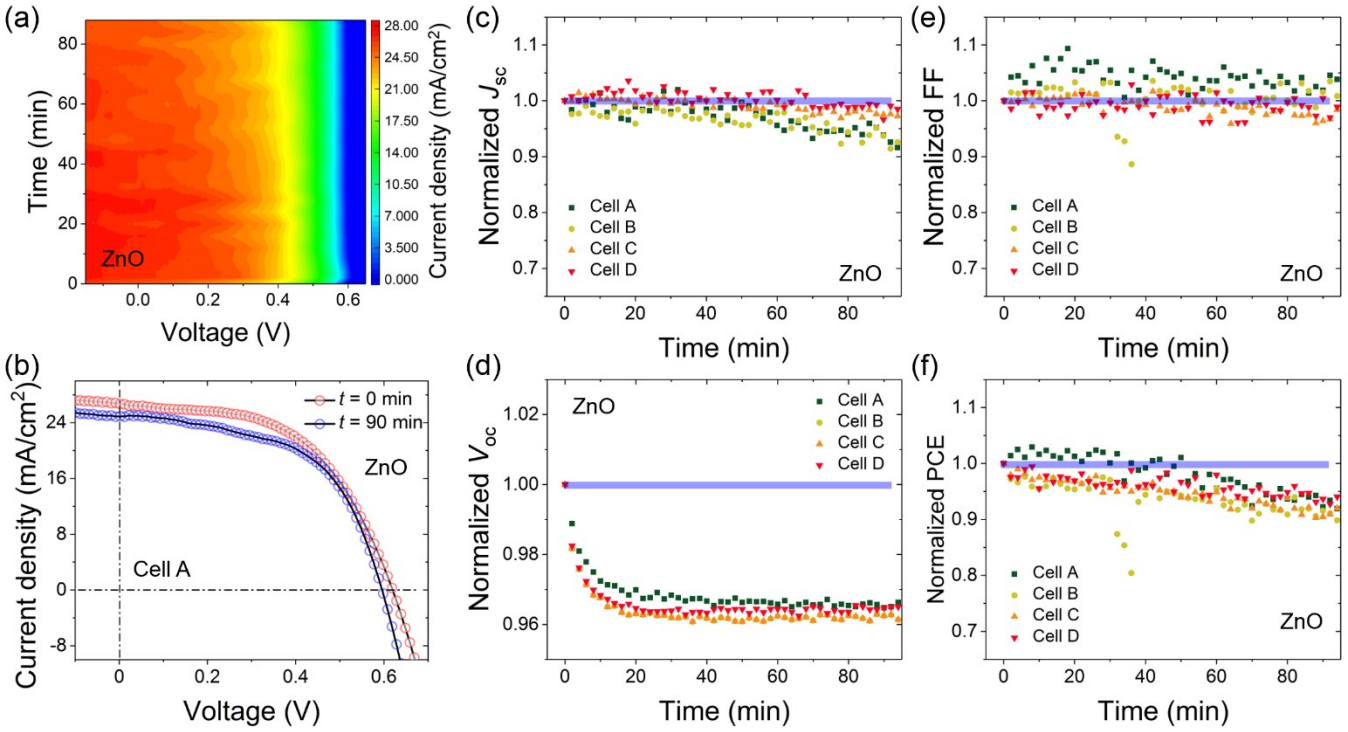

Fig. S9 (a) 2D J-V curve mapping of ZnO based solar cell during the degradation process. (b) The *J-V* curves of the device before (0 min, red) and after (90 min, blue) the degradation. Evolution of normalized device parameters for (c) short circuit current density (J_{sc}), (d) open circuit voltage (V_{oc}), (e) fill factor (FF) and (f) power conversion efficiency (PCE), in which the Cell B, C, D are fabricated as reference samples demonstrating a similar degradation tendency compared to Cell A.

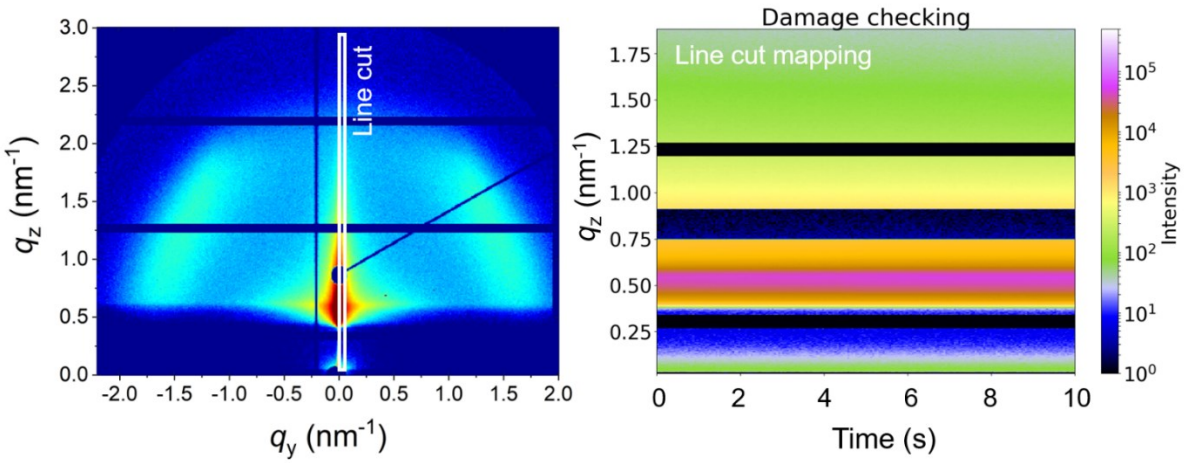

Fig. S10 Radiation damage test before the *operando* experiment, in which the X-ray illuminates on a selected position (not the *operando* position) for 0.1 s * 100, which is longer than the total exposure time 0.5 s * 19 chosen for the *operando* experiment. The line cut is indicated in the 2D GISAXS data (left) and the line-cut mapping (right) records the structure evolution over the operation time. Potential radiation damage from the X-ray exposure is ruled out for all studies performed in this work.

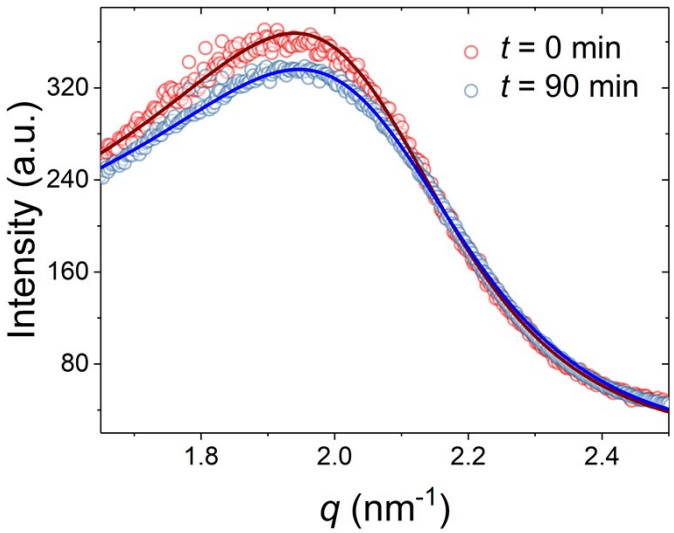

Fig. S11 Azimuthal integrations of 2D GISAXS data (symbols) of the solar cell before (0 min, red) and after degradation (90 min, blue) are shown with the best model fits (solid lines) using a model as described in the text.

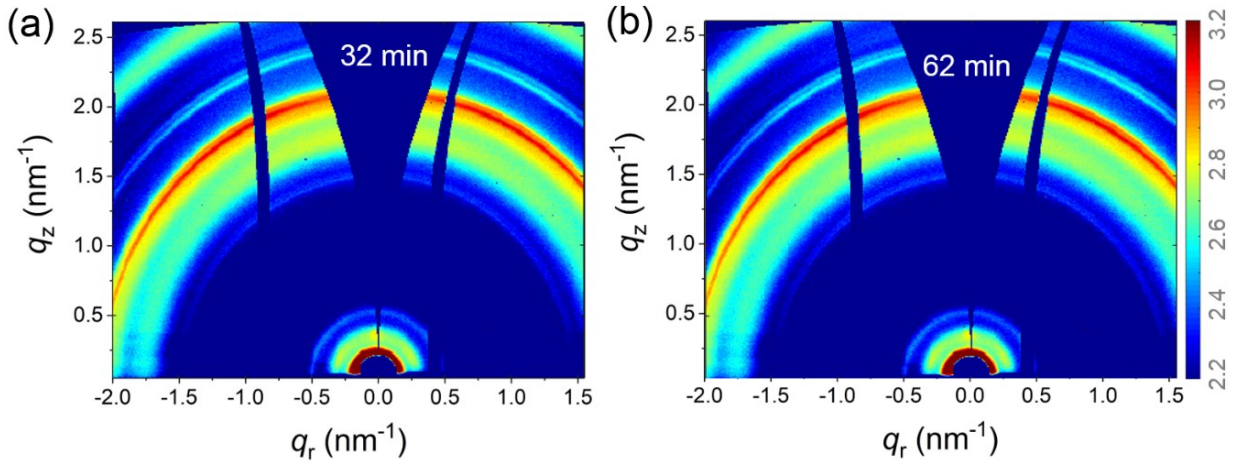

Fig. S12 2D GIWAXS data at (a) *t* = 32 min and (b) *t* = 62 min of illumination probed during the *operando* experiment.

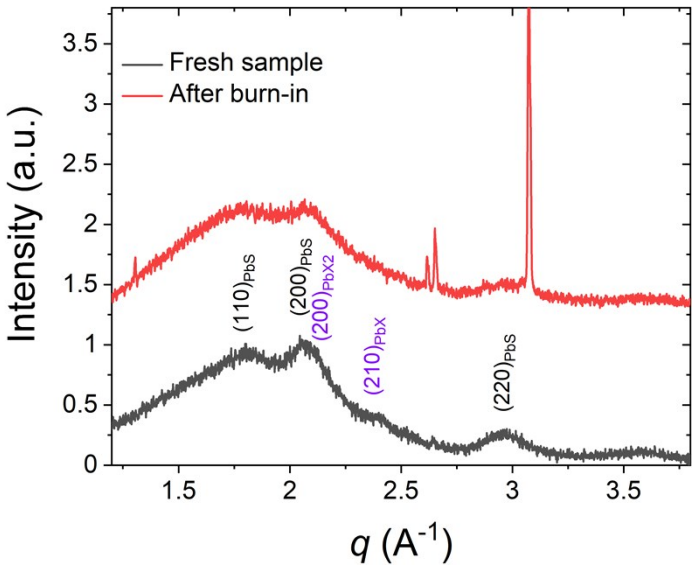

Fig. S13 XRD data of the fresh bare QD-ink layer on glass (black line), in which the $(200)_{PbS}$ and $(200)_{PbX2}$ peaks are merged. The existence of PbX2 crystals can be seen from the $(210)_{PbX2}$ peak at q = 2.4 Å^{-1}, which matches well with the *operando* GIWAXS data. XRD data of the QD-ink layer after the burn-in test (red line) show new crystalline peaks emerging, which are assigned to the PbX_2 component.

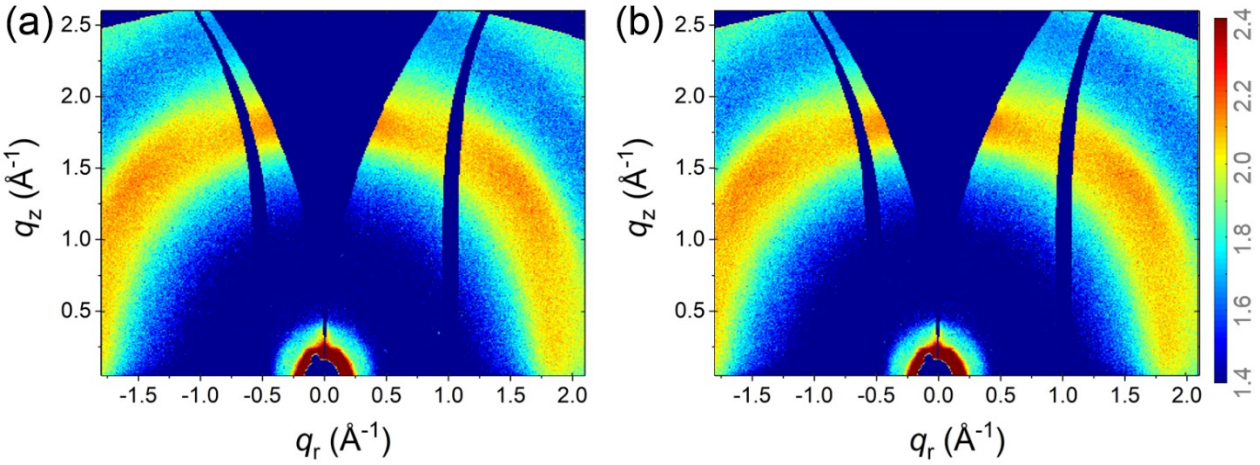

Fig. S14 Static 2D GIWAXS data of the bare EDT-QD layer (a) before and (b) after degradation.

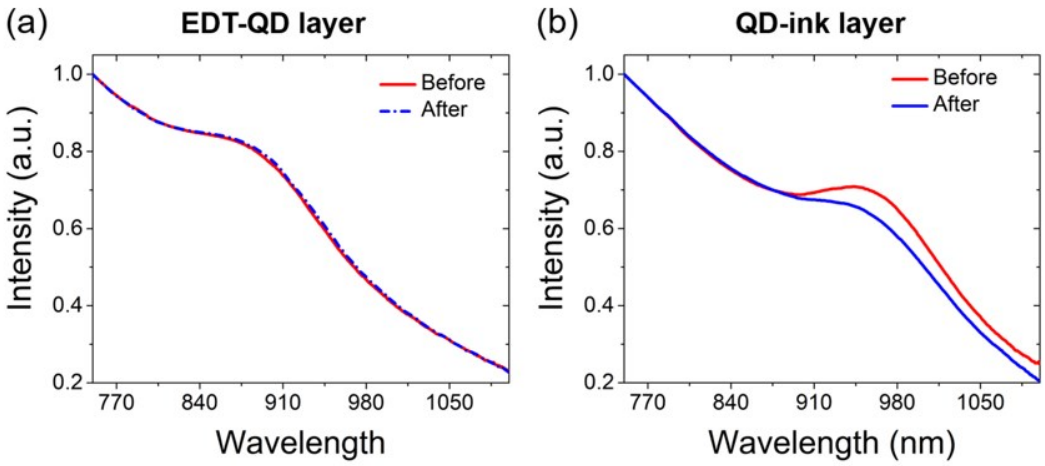

Fig. S15 Absorption spectra of (a) EDT-QD layer and (b) QD-ink layer on glass substrates before (red) and after (blue) the burn-in experiment.

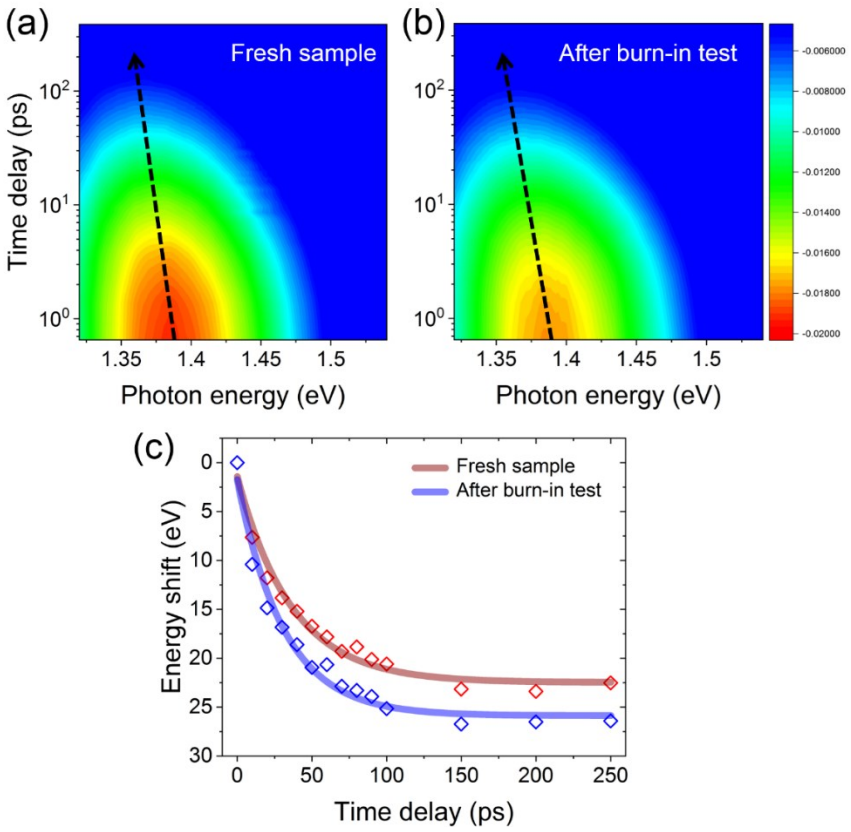

Fig. S16 Time-resolved bleaching mapping of 1Se-1Sh state under 10 mW pump fluence for (a) fresh sample and (b) aged sample under burn-in test conditions. (c) Energy shifts of the QD solid represented by the shift of the bleaching peak position. The curves are fitted with an exponential decay function (solid lines).

Table S1. Parameters of quantum dots solar cells used for SCAPS simulations

	QD-ink	PbS-EDT	ZnO
Thickness (nm)	230	50	80
Bandgap (eV)	1.14	1.14	3.35
Electron affinity (eV)	4.0	3.9	4
Dielectric permittivity	20	20	66
CB effective density of states (1/cm^3)	10^{19}	10^{19}	10^{19}
VB effective density of states (1/cm^3)	10^{19}	10^{19}	10^{19}
Electron thermal velocity (cm/s)	10^7	10^7	10^7
Hole thermal velocity (cm/s)	10^7	10^7	10^7
Electron mobility (cm^2/V·s)	2×10^{-2}	210^{-4}	510^{-2}
Hole mobility (cm^2/V·s)	2×10^{-2}	210^{-4}	510^{-2}
Shallow uniform donor density N_D (1/cm^3)	10^{15}	10^{14}	10^{17}
Shallow uniform acceptor density N_A (1/cm^3)	10^{15}	10^{16}	0

Table S2. Parameters of interfaces

Interfaces	PbS-EDT / QD-ink	QD-ink / ZnO
Charge type	neutral	neutral
Total density	10^{16}	2×10^{14}
Capture cross section electrons	1.2×10^{-13}	10^{-19}
Capture cross section holes	1.2×10^{-13}	10^{-19}

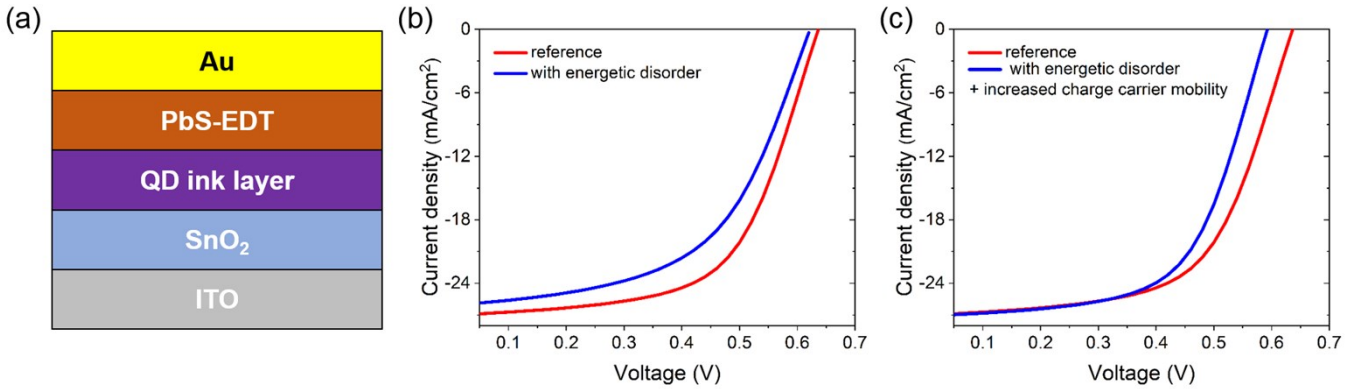

Fig. S17 (a) Sketch of the device architecture used for the SCAPS simulation. (b) Simulated JV curves with different energy disorders and (c) JV curves with additionally increased charge carrier mobilities, which are in very good agreement with measured device data shown in Fig. S5.

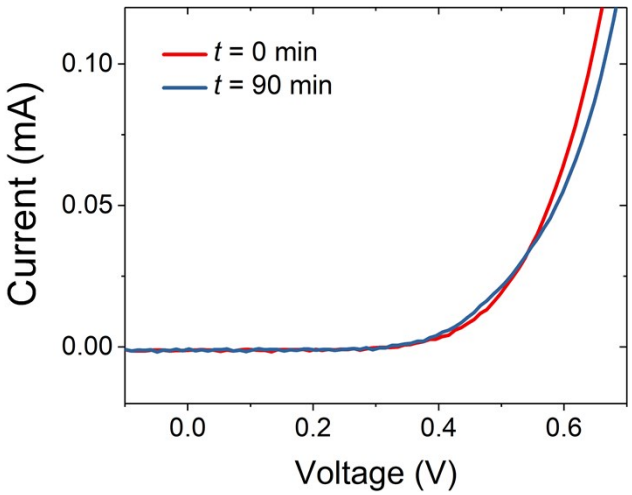

Fig. S18. Dark JV measurements of cell A (SnO_2 based device) before (*t* = 0 min, red) and after (*t* = 90 min, blue) the *operando* experiment.